Spacing distributions for real symmetric 2 × 2 generalized Gaussian ensembles



2009 J. Phys. A: Math. Theor. 42 485102

(http://iopscience.iop.org/1751-8121/42/48/485102)

IOP PUBLISHING JOURNAL OF PHYSICS A: MATHEMATICAL AND THEORETICAL

J. Phys. A: Math. Theor. **42** (2009) 485102 (13pp) doi:10.1088/1751-8113/42/48/485102

# Spacing distributions for real symmetric 2 × 2 generalized Gaussian ensembles

**M V Berry**[1] **and P Shukla**[2]

[1] H H Wills Physics Laboratory, Tyndall Avenue, Bristol BS8 1TL, UK
[2] Department of Physics, Indian Institute of Technology, Kharagpur, India

Received 11 August 2009
Published 12 November 2009
Online at stacks.iop.org/JPhysA/42/485102

**Abstract**
For ensembles of 2 × 2 real symmetric matrices, the normalized spacing distributions $P(S)$ form a family whose parameter space is the unit cube with coordinates determined by the means and variances of the diagonal and off-diagonal elements. The cube contains a variety of spacing distributions that are calculated analytically; they include the Wigner–Poisson transition, distributions with singularities and Gaussians. Unfolding is superfluous for 2 × 2 matrices, but it can be implemented, giving rise to a further variety of spacing distributions, some surprising.

PACS numbers: 02.70.rr, 02.65.−w, 05.45.mt

## 1. Introduction

2 × 2 matrices are useful models for many phenomena, including lens and polarization optics [1, 2], geometric phases [3], PT symmetry [4], quantum transitions [5–7], decoherence [8] and localization [9, 10]. Sometimes, the physics involves individual matrices, but more frequently insight is gained by considering *families* of matrices, for example those surrounding and including a degenerate matrix, where, for two parameters, the spectrum possesses a conical (diabolical) singularity [11]. In addition, average short-range spectral properties of statistical *ensembles* of $N \times N$ matrices can be illuminated by 2 × 2 examples [12].

Here we will study families of ensembles of 2 × 2 real symmetric matrices whose elements are independently Gauss-distributed, and we will calculate the unique fluctuation statistic for this family, namely the probability distribution $P(S)$ of the difference between the two eigenvalues, normalized so that $S$ is measured in units of the mean spacing. In the most familiar individual ensemble in this family, the elements have zero mean and the variance of the diagonal elements is twice that of the off-diagonals; this represents the 2 × 2 Gaussian orthogonal ensemble (GOE), and the spacing distribution, known as the Wigner surmise [12] of random-matrix theory, is a good approximation to that for $N \times N$ matrices when $N \gg 2$.

In the generalized ensembles we consider here, the diagonal and off-diagonal elements have arbitrary means and variances, and these quantities are the parameters of the family. We

  

will find that there are three such parameters, and individual ensembles correspond to points in a unit cube. In section 2 we calculate $P(S)$ for any point in the cube, and in section 3 we explore special cases, corresponding to particular edges and faces.

For a spectrum of just two eigenvalues, the unfolding procedure that is necessary for larger matrices [13] is superfluous, because $P(S)$ can be calculated directly. Nevertheless, unfolding is interesting to explore for $2 \times 2$ matrices (section 4), not only for comparison with larger matrices but also because it leads to some unexpected results: for traceless matrices, the unfolded spacing distribution is uniform on $0 < S < 2$, whatever the statistics of the matrix elements.

There are several reasons for studying the $2 \times 2$ model. (i) The matrices in these ensembles are caricatures of larger matrices more general than those of the GOE that have been widely applied in condensed-matter physics [14–17] and in studies of complexity [18–22]. (ii) It gives the simplest models for the spacing distribution, which is the statistic most commonly measured experimentally. (iii) Only for $2 \times 2$ matrices it is possible to carry out detailed analytical calculations. (iv) It is possible to study the complete parameter space, in contrast to larger matrices where there are many more parameters. (v) Even this simple generalization of the Wigner surmise displays a variety of spacing distributions.

In the following, we denote all probability distributions by $P$, distinguished by the variables appearing in its argument; thus $P(a)\,\mathrm{d}a = P(b)\,\mathrm{d}b$.

## 2. Calculation of the spacing distribution

The most general real symmetric matrix is

$$\mathbf{M} = \frac{1}{2}\begin{pmatrix} T+X & Y \\ Y & T-X \end{pmatrix}. \tag{2.1}$$

The spacing of the two eigenvalues $\lambda_+$ and $\lambda_-$, namely

$$\Delta = \lambda_+ - \lambda_- = \sqrt{X^2+Y^2}, \tag{2.2}$$

does not involve the trace $T$, which therefore plays no part in the direct calculation of the spacing distribution carried out in this section and the next. However, $T$ will reappear in section 4 when we discuss the distribution of spacings for unfolded eigenvalues.

If we choose the elements $X$ and $Y$ to be Gauss-distributed and uncorrelated, with means and variances

$$\bar{X},\ V_X,\ \bar{Y},\ V_Y, \tag{2.3}$$

these four quantities are the parameters of the ensemble before normalization.

The distribution of unnormalized spacings is

$$P(\Delta;\bar{X},\bar{Y},V_X,V_Y) = \frac{1}{2\pi\sqrt{V_X V_Y}}\int_{-\infty}^{\infty}\mathrm{d}X\int_{-\infty}^{\infty}\mathrm{d}Y\,\delta(\Delta-\sqrt{X^2+Y^2}) \times \exp\left\{-\left(\frac{(X-\bar{X})^2}{2V_X}+\frac{(Y-\bar{Y})^2}{2V_Y}\right)\right\}. \tag{2.4}$$

It is convenient to introduce polar coordinates for $X$, $Y$, and integrate over the radial coordinate. Then we scale to introduce the following natural dimensionless parameters and new temporary spacing variable:

$$\xi \equiv \frac{\bar{X}}{(V_X V_Y)^{1/4}}, \qquad \eta \equiv \frac{\bar{Y}}{(V_X V_Y)^{1/4}}, \qquad \alpha \equiv \sqrt{\frac{V_x}{V_Y}}, \qquad D \equiv \frac{\Delta}{(V_X V_Y)^{1/4}}. \tag{2.5}$$

In terms of $D$, the resulting spacing distribution now depends on only three parameters:

$$P(D;\xi,\eta,\alpha)=\frac{D}{2\pi}\exp\left(-\left(\frac{\xi^2}{2\alpha}+\frac{\eta^2\alpha}{2}\right)\right)\times\int_0^{2\pi}\mathrm{d}\theta\exp\left(-\frac{D^2}{2}\left(\frac{\cos^2\theta}{\alpha}+\alpha\sin^2\theta\right)+D\left(\xi\frac{\cos\theta}{\alpha}+\alpha\eta\sin\theta\right)\right).\quad(2.6)$$

Finally, we scale $D$ by the mean spacing, which is

$$\bar{D}(\xi,\eta,\alpha)=\int_0^\infty \mathrm{d}D\,DP(D)=\frac{\exp\left(-\left(\frac{\xi^2}{2\alpha}+\frac{\alpha\eta^2}{2}\right)\right)}{2\sqrt{2\pi}}\times\int_0^{2\pi}\mathrm{d}\theta\frac{\left[A+(1+A^2)\exp\left(\frac{1}{2}A^2\right)\left(1+\mathrm{erf}\left(\frac{A}{\sqrt{2}}\right)\right)\right]}{\left(\frac{\cos^2\theta}{\alpha}+\alpha\sin^2\theta\right)^{3/2}},\quad(2.7)$$

where

$$A=\frac{\frac{\xi}{\alpha}\cos\theta+\alpha\eta\sin\theta}{\sqrt{\frac{\cos^2\theta}{\alpha}+\alpha\sin^2\theta}}.\quad(2.8)$$

Thus, the desired spacing distribution is

$$P(S;\xi,\eta,\alpha)=\frac{S(\bar{D}(\xi,\eta,\alpha))^2}{2\pi}\exp\left(-\left(\frac{\xi^2}{2\alpha}+\frac{\eta^2\alpha}{2}\right)\right)\times\int_0^{2\pi}\mathrm{d}\theta\exp\left(F(\theta;S,\xi,\eta,\alpha)\right),\quad(2.9)$$

where

$$F(\theta;S,\xi,\eta,\alpha)=\frac{S^2(\bar{D}(\xi,\eta,\alpha))^2}{2}\left(\frac{\cos^2\theta}{\alpha}+\alpha\sin^2\theta\right)+S\bar{D}(\xi,\eta,\alpha)\left(\xi\frac{\cos\theta}{\alpha}+\alpha\eta\sin\theta\right).\quad(2.10)$$

The spacing distribution is invariant under each of the replacements $\xi\to-\xi$, $\eta\to-\eta$, $\{\alpha,\xi,\eta\}\to\{\alpha^{-1},\eta,\xi\}$. Incorporating these symmetries, the ranges of the three parameters are

$$0<\xi<\infty,\qquad 0<\eta<\infty,\qquad 0\leqslant\alpha\leqslant 1,\quad(2.11)$$

corresponding to an infinite square $(\xi,\eta)$ slab with unit height $(\alpha)$. With coordinates $\tanh\xi$ and $\tanh\eta$, this parameter space becomes the unit cube (figure 1), in which each point represents one of the generalized Gaussian ensembles.

## 3. Special cases

*Case A. Both means zero* ($\bar{X}=\bar{Y}=0$)*, arbitrary variances*

This is $\xi=\eta=0$, so the only parameter is $\alpha$ (see figure 1). Equations (2.7) and (2.9) simplify considerably; the quantity $A$ in (2.8) is zero, and $\bar{D}$ can be expressed in terms of hypergeometric functions:

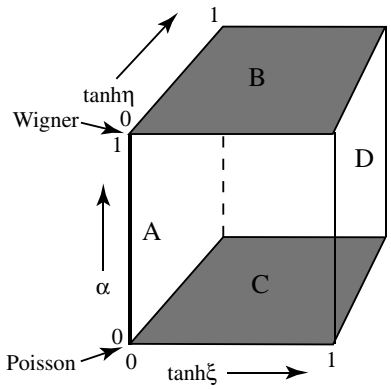


**Figure 1.** Parameter cube of the family of ensembles, indicating the special cases treated in section 3.

$$\bar{D}(\alpha,0,0) = \frac{1}{2\sqrt{2\pi}}\int_0^{2\pi} \mathrm{d}\theta \frac{1}{\left(\frac{\cos^2\theta}{\alpha}+\alpha\sin^2\theta\right)^{3/2}}$$
$$= \frac{2\sqrt{\pi}}{(\alpha^{-1}+\alpha)^{3/2}}\,{}_2F_1\left(\frac{3}{4},\frac{5}{4},1,\frac{(\alpha^{-1}-\alpha)^2}{(\alpha^{-1}+\alpha)^2}\right) \approx \sqrt{\frac{2}{\pi}(\alpha^{-1}+\alpha)+\frac{(\pi-8/\pi)}{(\alpha^{-1}+\alpha)}}, \tag{3.1}$$

in which the approximation in the last member is exact as $\alpha \to 0$ and $\alpha \to 1$ and the error never exceeds 1.5% over the entire range of $\alpha$.

$P(S)$ (equation (2.9)) is simple too: in terms of the Bessel function $I_0$,

$$P(S;\alpha,0,0) = S\bar{D}(\alpha,0,0)^2\exp\left\{-\tfrac{1}{4}S^2\bar{D}\,(\alpha,0,0)^2\,(\alpha+1/\alpha)\right\}$$
$$\times I_0\left(\tfrac{1}{4}S^2\bar{D}(\alpha,0,0)^2(\alpha-1/\alpha)\right). \tag{3.2}$$

This special case has been derived before [23], and described as the quadratic Rayleigh–Rice distribution.

A familiar limiting case is where both variances are equal; then

$$P(S;1,0,0) = \frac{\pi}{2}S\exp\left(-\frac{1}{4}\pi S^2\right), \tag{3.3}$$

reproducing the familiar Wigner surmise, displaying linear eigenvalue repulsion (as do all the ensembles, except one that will be considered later in this section). The fact that (3.3) corresponds to equal variances for the diagonal and off-diagonal elements might seem unfamiliar. But if $T$ in (2.1) has variance $V_T = V_X = V_Y$, the variance of the diagonal elements is

$$V_{\mathrm{diag}} = V_{T+X} = V_{T-X} = V_T + V_X = 2V_X, \tag{3.4}$$

explaining the factor 2 in the usual formulations.

The opposite limit is $\alpha = 0$, for which

$$P(S;0,0,0) = \frac{2}{\pi}\exp\left(-\frac{1}{\pi}S^2\right). \tag{3.5}$$

Since this corresponds to a purely diagonal matrix, $P(S;0,0,0)$ is simply the distribution of distances between two independent Gauss-distributed numbers, that is, the equivalent of

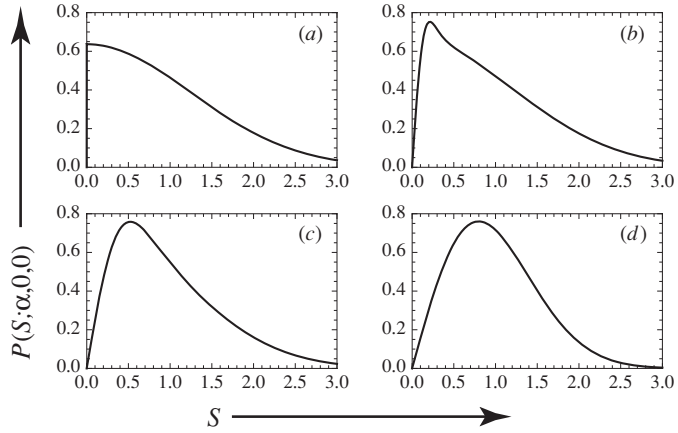


**Figure 2.** Spacing distribution $P(S;\alpha,0,0)$ (equation (3.2)) for (*a*) $\alpha = 0$ (Poisson), (*b*) $\alpha = 0.1$, (*c*) $\alpha = 0.3$, (*d*) $\alpha = 1$ (Wigner).

the Poisson distribution for $2 \times 2$ matrices, displaying no eigenvalue repulsion (the familiar exponential distribution emerges for diagonal $N \times N$ matrices as $N$ increases).

Thus, the spacing distribution (3.2) represents an interpolation between the Poisson and Wigner ensembles, as illustrated in figure 2. By choosing a non-Gaussian ensemble for the diagonal elements, it is possible [24, 25] to reproduce the familiar exponential form for the Poisson distribution for large matrices, but for $2 \times 2$ matrices the exponential form has no special status: only the lack of eigenvalue repulsion is significant.

*Case B. Both variances equal ($V_X = V_Y$), arbitrary means*

This is the $\alpha = 1$ face of the parameter cube (see figure 1). The parameters $\xi$ and $\eta$ appear only in the combination

$$\rho = \sqrt{\xi^2 + \eta^2}, \tag{3.7}$$

and (2.7) and (2.9) give

$$\bar{D}(1, \sqrt{\xi^2+\eta^2} = \rho) = \frac{1}{2}\sqrt{\frac{\pi}{2}} \exp\left(-\frac{1}{4}\rho^2\right)\left[(2+\rho^2) I_0\left(\frac{1}{4}\rho^2\right) + \rho^2 I_1\left(\frac{1}{4}\rho^2\right)\right], \tag{3.8}$$

and

$$P(S; 1, \sqrt{\xi^2+\eta^2} = \rho) = S\bar{D}(\rho)^2 \exp\left\{-\tfrac{1}{2}(\rho^2 + S^2\bar{D}(\rho)^2)\right\} I_0(S\rho\bar{D}(\rho)). \tag{3.9}$$

This looks similar to the quadratic Rayleigh–Rice distribution in (3.2) of case A but is in fact very different (except for $\rho = 0$) because the Bessel function involves $S$ rather than $S^2$; it is the ordinary Rice distribution.

Figure 3 shows $P(S; 1, \sqrt{\xi^2+\eta^2} = \rho)$ for several values of $\rho$. Now the transition is very different: from Wigner at $\rho = 0$ via a Gaussian sharpening to a $\delta$ function:

$$P(S, 1, \sqrt{\xi^2+\eta^2} = \rho \to \infty) \to \frac{\rho}{\sqrt{2\pi}} \exp\left(-\tfrac{1}{2}\rho^2(S-1)^2\right) \to \delta(S-1). \tag{3.10}$$

This limit is obvious, because if either mean is much larger than the common variance, then the spacing distribution before normalization by the mean spacing is a Gaussian centred on a large spacing, which when normalized gives $P(S)$ as a narrow Gaussian centred on $S = 1$, corresponding to a rigid spectrum.

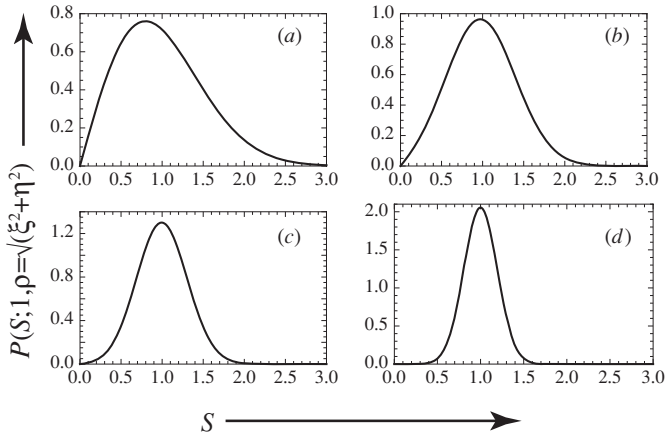


**Figure 3.** Spacing distribution $P(S;1,\sqrt{\xi^2+\eta^2}=\rho)$ (equation (3.9)) for (*a*) $\rho=0$ (Wigner), (*b*) $\rho=2$, (*c*) $\rho=3$, (*d*) $\rho=5$.

*Case C. One variance zero, arbitrary means*

Without loss of generality we can choose $V_X$ as the zero variance. Then from (2.5) this case corresponds to $\alpha=0, \xi=\eta=\infty$ (see figure 1). However, it is easier to return to (2.4) and note the simplification that this case is simply $X=\bar{X}$, i.e. the $X$ distribution is a $\delta$ function, so

$$P(\Delta)=\frac{1}{\sqrt{2\pi V_Y}}\int_{-\infty}^{\infty}\mathrm{d}Y\,\delta(\Delta-\sqrt{\bar{X}^2+Y^2})\exp\left\{-\tfrac{1}{2}\left(\frac{(Y-\bar{Y})^2}{V_Y}\right)\right\}$$
$$=\frac{\Theta(\Delta-\bar{X})2\Delta}{\sqrt{2\pi V_Y(\Delta^2-\bar{X}^2)}}\exp\left\{-\left(\frac{\Delta^2-\bar{X}^2+\bar{Y}^2}{2V_Y}\right)\right\}\cosh\left(\frac{\bar{Y}}{V_Y}\sqrt{\Delta^2-\bar{X}^2}\right), \tag{3.11}$$

in which $\Theta$ denotes the unit step. Now there are two new natural parameters and a new natural temporary spacing variable:

$$\xi_1\equiv\frac{\bar{X}}{\sqrt{V_Y}}=\sqrt{\alpha}\xi,\qquad \eta_1\equiv\frac{\bar{Y}}{\sqrt{V_Y}}=\sqrt{\alpha}\eta,\qquad D_1\equiv\frac{\Delta}{\sqrt{V_Y}}=\sqrt{\alpha}D. \tag{3.12}$$

The mean spacing is

$$\bar{D}_1(\xi_1,\eta_1)=\sqrt{\frac{2}{\pi}}\exp\left(-\frac{1}{2}\eta_1^2\right)\int_0^{\infty}\mathrm{d}\tau\sqrt{\tau^2+\xi_1^2}\exp\left(-\frac{1}{2}\tau^2\right)\cosh(\tau\eta_1)$$
$$\approx\sqrt{\frac{2}{\pi}+\xi_1^2+\eta_1^2}, \tag{3.13}$$

in which the approximation is exact for $\xi_1=\eta_1=0$ and as $\xi_1\to\infty$ or $\eta_1\to\infty$, and the error never exceeds 9%. The spacing distribution is (in an obvious notation)

$$P(S;0,\xi_1,\eta_1)=\frac{\Theta(S-|\xi_1|/\bar{D}_1(\xi_1,\eta_1))2S\bar{D}_1(\xi_1,\eta_1)^2}{\sqrt{2\pi(S^2\bar{D}_1(\xi_1,\eta_1)^2-\xi_1^2)}}$$
$$\times\exp\left\{-\frac{1}{2}(S^2\bar{D}_1(\xi_1,\eta_1)^2-\xi_1^2+\eta_1^2)\right\}\cosh\left(\eta_1\sqrt{S^2\bar{D}_1(\xi_1,\eta_1)^2-\xi_1^2}\right). \tag{3.14}$$

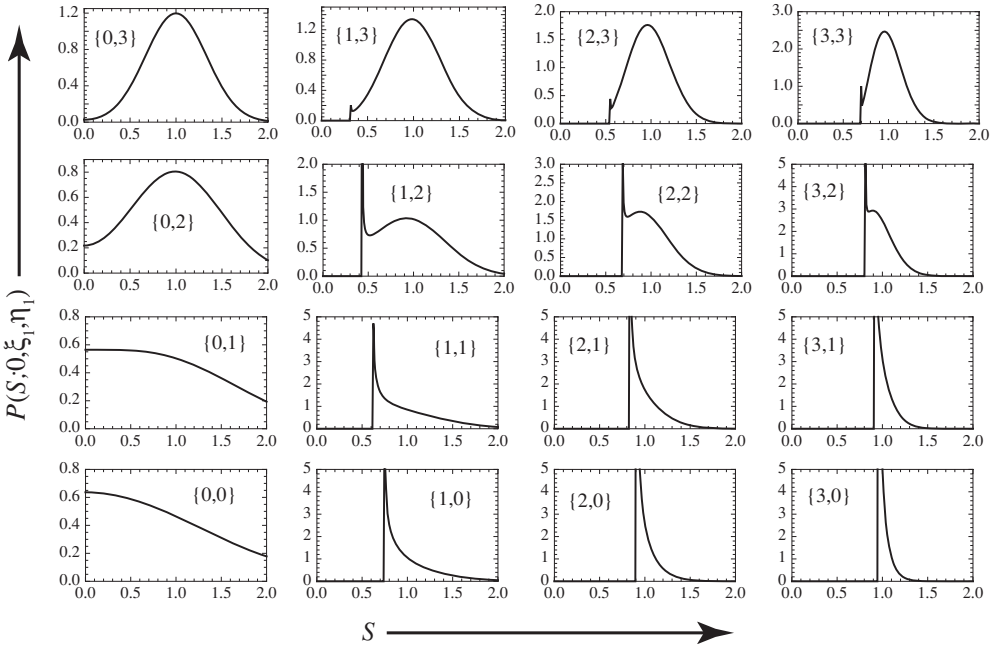


**Figure 4.** Spacing distribution $P(S; 0, \xi_1, \eta_1)$ (equations (3.12)–(3.14)), for the indicated values of $\{\xi_1, \eta_1\}$.

Figure 4 shows the variety of spacing distributions that can be generated by different choices of the parameters $\xi_1$ and $\eta_1$. The distributions possess singularities at $S_c = \xi_1/D_1(\xi_1, \eta_1)$, with $S_c \approx \xi_1/\sqrt{\xi_1^2 + \eta_1^2}$ for large $\xi_1$ or $\eta_1$. In addition, there are maxima close to $S = S_c\sqrt{1 + \eta_1^2/\xi_1^2}$; these maxima get larger and narrower as $\xi_1$ or $\eta_1$ increase, leading in the limit to the rigid spectrum distribution $\delta(S-1)$ (cf (3.10)).

*Case D.* $|\xi|$ *and/or* $|\eta| \gg 1$

This corresponds to the two means being much greater than the variances (see figure 1). Then we expect the scaled spacings $D$ (equation (2.5)) to be concentrated near $\xi^2 + \eta^2$. In the integral (2.9), the exponent is a rapidly varying function of $\theta$, whose stationary point is close to $\theta = \arctan(\eta/\xi)$. Straightforward but tedious algebra then leads to the spacing distribution

$$P(S; \alpha, \xi, \eta) \approx \frac{(\xi^2 + \eta^2)}{\sqrt{2\pi\left(\alpha\xi^2 + \frac{\eta^2}{\alpha}\right)}} \exp\left\{-\frac{(\xi^2 + \eta^2)^2(S-1)^2}{2\left(\alpha\xi^2 + \frac{\eta^2}{\alpha}\right)}\right\} \qquad \text{if} \quad \xi^2 + \eta^2 \gg 1. \tag{3.15}$$

This approximation is a Gaussian with rms width

$$\frac{\sqrt{\left(\alpha\xi^2 + \frac{\eta^2}{\alpha}\right)}}{(\xi^2 + \eta^2)}, \tag{3.16}$$

getting narrower as $\xi^2 + \eta^2$ increases, again leading to the limiting rigid spectrum distribution $\delta(S-1)$.

## 4. Unfoldings

The normalization we have used—demanding that the mean spacing $\bar{S} = 1$—looks different from the usual unfolding procedure [13], in which $S = \Delta d(\lambda)$, where $d(\lambda)$ is the mean eigenvalue density for eigenvalues near $\lambda$. But the usual procedure is intended to apply to large matrices, where $d(\lambda)$ varies very slowly on the scale of the spacings $\Delta$, so the unfolding is equivalent to the requirement $\bar{S} = 1$. By contrast, in our $2 \times 2$ case, $d(\lambda)$ varies considerably on the scale $\Delta$, so the usual procedure (which involves $\lambda$) is ambiguous. Moreover, it is superflous, because we can impose $\bar{S} = 1$ directly. Nevertheless, it is interesting to explore unfolding, because some of the resulting distributions are unexpected.

The eigenvalues of the matrix (2.1) are

$$\lambda_\pm = \tfrac{1}{2}(T \pm R), \tag{4.1}$$

where $R \equiv \sqrt{X^2 + Y^2}$. Then the mean level density is

$$d(\lambda) = \int_{-\infty}^{\infty} \mathrm{d}T\, P\,(T) \int_{-\infty}^{\infty} \mathrm{d}X\, P\,(X) \int_{-\infty}^{\infty} \mathrm{d}Y\, P\,(Y) \times \left[\delta\left(\lambda - \frac{1}{2}(T - R)\right) + \delta\left(\lambda - \frac{1}{2}(T + R)\right)\right]. \tag{4.2}$$

Noting that $|\lambda - T/2| = \Delta/2$, the density can be expressed in terms of the spacing distribution (2.4) before scaling, smoothed by the distribution of the trace $T$:

$$d\,(\lambda) = 2\int_{-\infty}^{\infty} \mathrm{d}\Delta\; P\,(T = \Delta + 2\lambda)\; P\,(|\Delta|)\,. \tag{4.3}$$

The associated level counting function,

$$N\,(\lambda) = \int_{-\infty}^{\lambda} \mathrm{d}\lambda' d\left(\lambda'\right), \tag{4.4}$$

increases from 0 to 2 as $\lambda$ increases from $-\infty$ to $+\infty$. A natural and convenient definition of the unfolded levels (though not the only possibility) is

$$\varepsilon_\pm \equiv N\,(\lambda_\pm)\,, \tag{4.5}$$

giving the local unfolded spacing $\sigma$ as a function of the spacing $\Delta$ before unfolding and the mean eigenvalue position $T/2$:

$$\sigma\,(\Delta; T) = \varepsilon_+ - \varepsilon_- = \int_{\frac{1}{2}(T-\Delta)}^{\frac{1}{2}(T+\Delta)} \mathrm{d}\lambda d\,(\lambda). \tag{4.6}$$

As $\Delta$ increases from $-\infty$ to $+\infty$ with $T$ fixed, $\sigma$ increases monotonically from 0 to 2. Therefore, the function $\sigma$ can be inverted to give $\Delta(\sigma; T)$, leading to the desired distribution of the local unfolded spacings, depending on $T$ as well as $\sigma$:

$$P(\sigma; T) = P(\Delta(\sigma; T)) \left|\frac{\mathrm{d}\Delta\,(\sigma; T)}{\mathrm{d}\sigma}\right| = \frac{2P(\Delta(\sigma; T))}{d\left(\frac{1}{2}(T + \Delta(\sigma; T))\right) + d\left(\frac{1}{2}(T - \Delta(\sigma; T))\right)}. \tag{4.7}$$

This distribution vanishes outside the interval $0 < \sigma < 2$.

The case of traceless matrices ($T = 0$) is particularly interesting. The distribution in (4.3) is $P(T) = \delta(T)$ and the level density is just the spacing distribution

$$d(\lambda) = 2P(\Delta = 2|\lambda|), \tag{4.8}$$

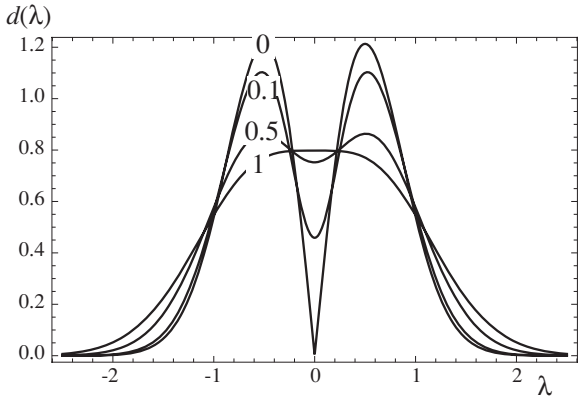


**Figure 5.** Level density (4.8) for the indicated values of the variance $V_T$ of the trace $T$ in (2.1).

which vanishes at $\lambda = 0$ because of level repulsion. Then the denominator in (4.7) cancels the numerator, and the spacing distribution is simply a constant:

$$P(\sigma; T = 0) = \left\{ \tfrac{1}{2} \text{ if } 0 < \sigma < 2, 0 \text{ if } \sigma > 2 \right\}. \tag{4.9}$$

This unexpected result holds for any traceless $2 \times 2$ matrices; the elements $X$ and $Y$ need not be Gauss-distributed, and may be correlated.

For matrices that are not traceless, we can take the distribution of $T$ to be Gaussian with variance $V_T$ and zero mean (a non-zero mean is trivially accommodated by a shift in $\lambda$). For $X$ and $Y$ it will suffice to consider the simplest case $\bar{X} = \bar{Y} = 0, V_X = V_Y = 1$, that is $\xi = \eta = 0, \alpha = 1$ in the notation of section 2, for which the spacing distribution is just the Wigner surmise (3.3). Then the level density (4.3) is

$$d(\lambda, V_T) = 2\sqrt{\frac{2V_T}{\pi}}\frac{\exp(-2\lambda^2/V_T)}{(1+V_T)} + \frac{4\lambda}{(1+V_T)^{3/2}}\sqrt{2}\lambda \times \exp\left(-\frac{2\lambda^2}{1+V_T}\right)\mathrm{Erf}\left(\lambda\sqrt{\frac{2}{V_T\,(1+V_T)}}\right). \tag{4.10}$$

Figure 5 illustrates how the density gets smoothed and broadened as $V_T$ increases from zero.

The unfolded local spacings are, from (4.6),

$$\sigma(\Delta; T, V_T) = \mathrm{Erf}\left(\frac{\Delta - T}{\sqrt{2V_T}}\right) + \mathrm{Erf}\left(\frac{\Delta + T}{\sqrt{2V_T}}\right) - \frac{1}{\sqrt{2}}\left(\mathrm{Erf}\left(\frac{\Delta - T}{\sqrt{2V_T(1+V_T)}}\right)\exp\left(-\frac{(\Delta - T)^2}{2(1+V_T)}\right) + \mathrm{Erf}\left(\frac{\Delta + T}{\sqrt{2V_T\,(1+V_T)}}\right)\exp\left(-\frac{(\Delta + T)^2}{2\,(1+V_T)}\right)\right). \tag{4.11}$$

Figures 6–8 show the corresponding local unfolded spacing distributions (4.7) for different values of the mean eigenvalue $T/2$ and variance $V_T$. It is clear that for these $2 \times 2$ matrices

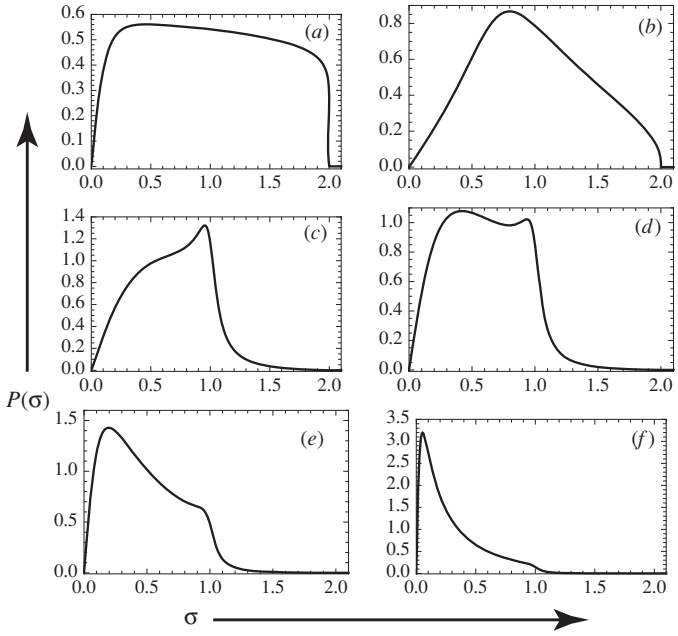


**Figure 6.** Unfolded local spacing distribution (4.7) for variance $V_T = 0.1$ and (*a*) $T = 0$, (*b*) $T = 0.7$, (*c*) $T = 2$, (*d*) $T = 2.2$, (*e*) $T = 2.5$, (*f*) $T = 3$.

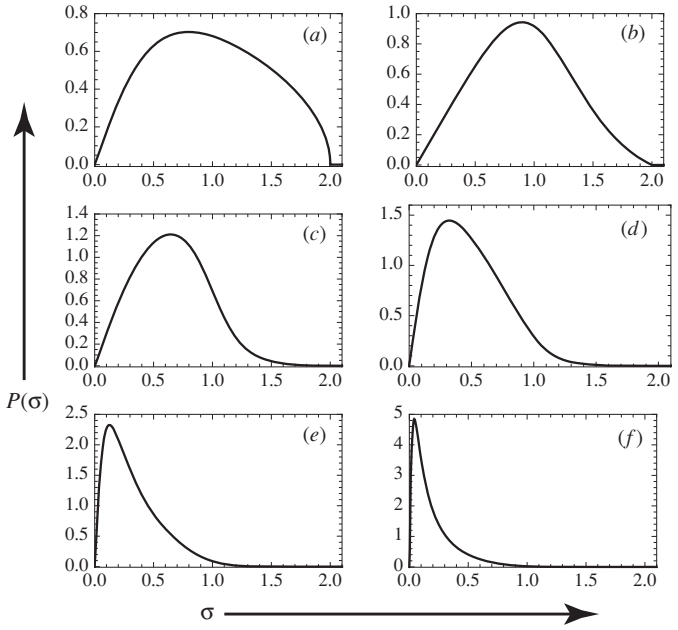


**Figure 7.** As figure 6, for $V_T = 0.5$ and (*a*) $T = 0$, (*b*) $T = 1$, (*c*) $T = 2$, (*d*) $T = 2.5$, (*e*) $T = 3$, (*f*) $T = 3.5$.

unfolding has introduced unnecessary complication, even in this simplest case where the direct averaging gives the unique Wigner surmise, independently of the distribution of $T$.

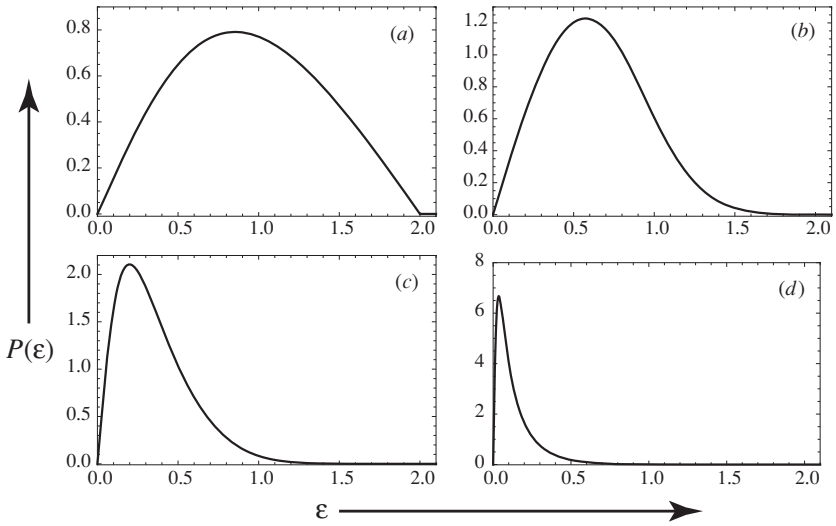


**Figure 8.** As figure 6, for $V_T = 1$ and (*a*) $T = 0$, (*b*) $T = 2$, (*c*) $T = 3$, (*d*) $T = 4$.

The complication can be reduced by averaging the local spacing distributions (4.7) over $T$, giving

$$P(\sigma; V_T) \equiv \int_0^\infty \mathrm{d}T\, P(\sigma; T, V) = \sqrt{\frac{2}{\pi V_T}} \int_0^\infty \mathrm{d}T \times \frac{\Delta(\sigma; T, V_T) \exp\left(-\frac{1}{2}\left(\frac{T^2}{V_T} + \Delta^2(\sigma; T, V_T)\right)\right)}{\left[d\left(\frac{1}{2}(T + \Delta(\sigma; T, V_T)), V_T\right) + d\left(\frac{1}{2}(T - \Delta(\sigma; T, V_T)), V_T\right)\right]}. \tag{4.12}$$

But, as figure 9 illustrates, the transition from the uniform distribution for $V_T = 0$ as $V_T$ increases still generates a variety of distributions. And for $V_T = 1$ (figure 9(*d*)), for which the distribution of matrix elements in (2.1) is the GOE, the unfolded distribution still differs substantially from the Wigner surmise that is such a good model for larger matrices.

It would be easy to evaluate (4.7) for matrices in the generalized ensembles considered in sections 2 and 3. This would augment the parameter cube by the additional parameters $T$ and $V_T$ and further complication as in the simplest case considered above.

## 5. Discussion

Of the six possible parameters labelling the general Gaussian statistics of $2 \times 2$ matrices—namely the means and variances of $T$, $X$ and $Y$ in (2.1)—only three—namely $\xi$, $\eta$ and $\alpha$, defined in (2.5)—are required to encompass all the spacing distributions. It is clear that this parameter family includes a rich variety of spacing distributions, in addition to the familiar stationary Wigner, Poisson and rigid distributions. Figures 2–4 illustrate this for the special cases considered in section 3, corresponding to points on the boundary of the parameter cube. Computations for points in the interior of the cube show similar spacing distributions. Particular single-parameter paths through the full parameter space have been found to be convenient models for wide classes of physical systems [26–29], though of course the properties of each ensemble are independent of whatever path is chosen to reach it.

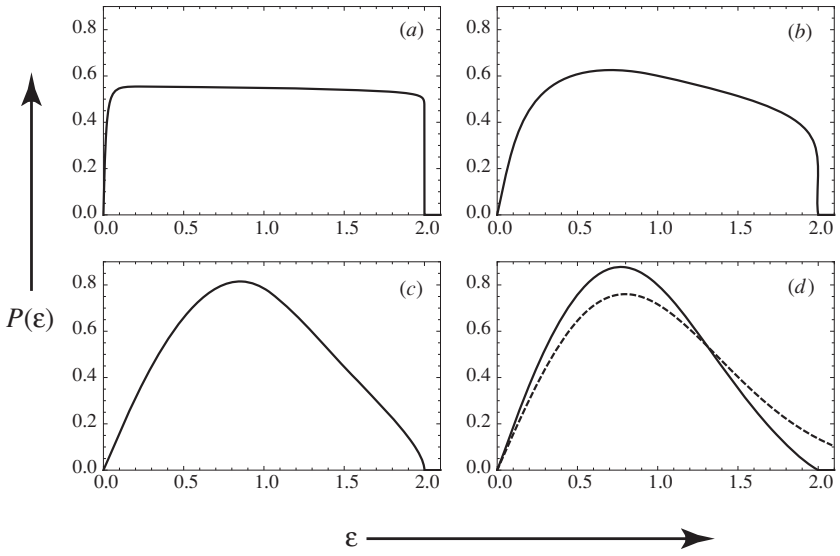


**Figure 9.** Average (4.10) of the local spacing distributions (4.7), for (*a*) $V_T = 0.001$, (*b*) $V_T = 0.1$, (*c*) $V_T = 0.5$, (*c*) $V_T = 1$. In (*d*) the dashed curve gives the Wigner surmise $\sigma \exp(-\frac{1}{2}\sigma^2)$.

Some of the $P(S)$ pictures appear to exhibit stronger-than-linear level replusion, and this is genuine in case C when $\xi_1 > 0$. Otherwise, the appearance of repulsion is illusory, for equation (2.9) shows that there is almost always linear repulsion, given precisely by

$$P(S;\alpha,\xi,\eta) \to S\bar{D}(\alpha,\xi,\eta)^2 \exp\left(-\left(\frac{\xi^2}{2\alpha}+\frac{\eta^2\alpha}{2}\right)\right) \qquad \text{as} \quad S \to 0. \tag{5.1}$$

In some cases, the coefficient is very small, generating the illusion of much stronger repulsion.

As discussed in section 4, the unfolding procedure employed to generate fluctuation statistics in larger matrices, whose purpose is to ensure that the mean spacing is unity, is unnecessary in the $2 \times 2$ case where this normalization can be implemented directly. Moreover, as figures 6–9 illustrate, unfolding for $2 \times 2$ matrices generates a variety of spacing distributions, even for the simplest case $\xi = \eta = 0$, $V_X = V_Y = 1$; none of these distributions reproduces the Wigner surmise (3.3).

The family of generalized ensembles considered here is the simplest. Further generalization, to $2 \times 2$ complex Hermitian ensembles, or to non-Hermitian ensembles, is straightforward but of course involves more parameters.

## Acknowledgments

We thank two referees for helpful suggestions. MVB's research is supported by the Leverhulme Trust.

## References

[1] Gerrard A and Burch J M 1975 *Introduction to Matrix Methods in Optics* (London: Wiley)
[2] Jones R C 1941 New calculus for the treatment of optical systems *J. Opt. Soc. Am.* **31** 488–93
[3] Berry M V 1984 Quantal phase factors accompanying adiabatic changes *Proc. R. Soc. Lond.* A **392** 45–57

[4] Bender C M, Berry M V and Mandilara A 2002 Generalized PT symmetry and real spectra *J. Phys. A: Math. Gen* **35** L467–71
[5] Landau L 1932 Zur Theorie der Energieubertragung II *Phys. Sov. Union* **2** 46–51
[6] Majorana E 1932 Atomi orientati in campo magnetico variabile *Nuovo Cimento* **9** 43–50
[7] Zener C 1932 Non-adiabatic crossing of energy levels *Proc. R. Soc. Lond.* A **137** 696–702
[8] Berry M V 1995 *Some Two-State Quantum Asymptotics* in *Fundamental Problems of Quantum Theory* ed D M Greenberger and A Zeilinger (*Ann. N.Y. Acad. Sci.* vol 255) pp 303–17
[9] Furstenberg H 1963 Non-commuting random-matrix products *Trans. Am. Math. Soc.* **108** 377–428
[10] Berry M V and Klein S 1997 Transparent mirrors: rays, waves and localization *Eur. J. Phys.* **18** 222–8
[11] Teller E 1937 The crossing of potential surfaces *J. Phys. Chem.* **41** 109–16
[12] Porter C E 1965 *Statistical Theories of Spectra: Fluctuations* (New York: Academic)
[13] Haake F 1991 *Quantum Signatures of Chaos* (Heidelberg: Springer)
[14] Sheleyansky D 1994 Coherent propagation of two-interacting particles in a random potential *Phys. Rev. Lett.* **73** 2607–711
[15] Fyodorov Y V and Mirlin A D 1991 Scaling properties of localization in random band matrices: a sigma-model approach *Phys. Rev. Lett* **67** 2405–09
[16] Mirlin A D, Fyodorov Y V, Dittes F-M, Quezada J and Seligman T H 1996 Transition from localized to extended eigenstates in the ensemble of power-law random banded matrices *Phys. Rev.* E **54** 3221–30
[17] Fyodorov J V, Chubykalo O A, Izraelev F M and Casati G 1996 Wigner random banded matrices with sparse structure: local spectral density of states *Phys. Rev. Lett.* **76** 1603–6
[18] Timme M, Geisel T and Wolf F 2006 Speed of synchronization in complex networks of neural oscillators: analytic results based on random matrix theory *Chaos* **6** 015108-1–15
[19] Luo F, Zhong J, Yang Y, Scheuermann R and Zhou J 2006 Application of random matrix theory to biological networks *Phys. Lett.* A **357** 420–3
[20] Kwapien J, Drozdz S and Ioannides A A 2000 Cross-hemisphere correlation matrices for signals received by auditory cortex of the brain *Phys. Rev.* E **62** 5557–64
[21] Plerou V, Gopikrishnan P, Ronenow B, Amaral L A N and Stanley H E 2000 Econophysics: financial time-series from a statistical point of view *Physica* A **279** 443–56
[22] Santhanam M S and Patra P K 2001 Statistics of atmospheric correlations *Phys. Rev.* E **64** 016102-1–7
[23] Huu-Tai P C, Smirnova N A and Isacker P V 2002 Generalized Wigner surmise for ($2 \times 2$) random matrices *J. Phys. A: Math. Gen* **35** L199–206
[24] Lenz G and Haake F 1991 Reliability of small matrices for large spectra with nonuniversal fluctuations *Phys. Rev. Lett.* **67** 1–4
[25] Caurier E, Grammaticos B and Ramani A 1990 Level repulsion near integrability: a random-matrix analogy *J. Phys. A: Math. Gen.* **23** 4903–9
[26] Shukla P 2000 Alternative techniques for complex spectra analysis *Phys. Rev.* E **62** 2098–113
[27] Shukla P 2007 Eigenfunction statistics of complex systems: a common mathematical formulation *Phys. Rev.* E **75** 051113-1–20
[28] Dutta R and Shukla P 2007 Complex systems with half-integer spins: symplectic ensembles *Phys. Rev.* E **76** 051124-1–11
[29] Shukla P 2008 Towards a common thread in complexity: an accuracy driven approach *J. Phys. A: Math. Theor.* **41** 304023